Structural Changes of Electrodic Materials in Electrochemical Cells Observed by in Situ Energy Dispersive X-ray Diffraction (EDXD)

V. Rossi Albertini* and P. Perfetti

Istituto di Struttura della Materia, CNR, Via del fosso del Cavaliere 100, 00133, Roma

F. Ronci and B. Scrosati

Dipartimento di Chimica, Universita' "La Sapienza", P.le Aldo Moro 5, 00148, Roma

Received June 2, 2000. Revised Manuscript Received September 19, 2000

The in situ observation of the structural changes induced in electrodic active materials upon cycling is commonly performed by angular dispersive X-ray diffraction (ADXD). Here an alternative approach based on the energy dispersive X-ray diffraction (EDXD) is described, together with its application to the study of the well-known $LiNi_{0.8}Co_{0.2}O_2$ cathode material. In the first part, we briefly describe the technique and its application to the in situ study of electrode materials. In the second part, we discuss how the experimental data have to be processed in order to separate the signal produced by the active material only from that of the other parts of the cell. In the third part, a dense sampling of the changing structure of $LiNi_{0.8}Co_{0.2}O_2$ during the first three charge−discharge cycles is shown in terms of the lattice parameters time evolution. The results confirm what was already reported in the literature on the behavior of similar materials, providing, at the same time, detailed information on the evolving structure. In fact, although the resolution of EDXD is lower than that of ADXD, the measurements have a good accuracy, which guarantees a small statistical scattering of the lattice parameters experimental points. This, together with the high sampling density, gives the points the aspect of almost continuous curves, whose features can be of interest in the study of electrodic materials.

1. Introduction

1.1. Electrodic Materials in Lithium-Ion Batteries. The new generation of rechargeable lithium-ion batteries plays a fundamental role in the technology of portable devices such as phones and lap tops.[1] The need for higher performance induced researchers to deepen their knowledge of the processes involving lithium uptake and release in the electrodic materials during the charge−discharge cycles.

The active electrodic materials in lithium-ion batteries can be divided in two groups: intercalation materials and alloys, the first group being the most frequently used.[2,3]

An intercalation material is an inorganic compound, mainly a lithiated transition-metal oxide or a carbonaceous material, capable of reversibly inserting and deinserting small ions (i.e., Li^+) in its crystalline structure in order to counterbalance the reduction and oxidation of the material (i.e., electron injection or removal). In this kind of process, the lithium ions retain their charged nature and the exchanged electrons vary the oxidation state of the transition-metal ions only. The structure of the intercalation compounds provides sites pathways arranged in channels or layers that allow the intercalating species to easily diffuse in the host lattice without drastic changes.[4]

The second group consists of metals and metal oxides that have been proposed as anodes (i.e., negative electrodes) for lithium-ion batteries thanks to their ability to form alloys with lithium. In this case, the lithium ion is reduced to metallic lithium to form an alloy with the metal electrode.[5]

In both of those cases, it is very important to study the structural variations that occur in the active material during the insertion/deinsertion process (i.e., upon cycling the battery). In this way, the possible presence of irreversible structural changes or of major volume variations, which can be responsible for limited capacity and cycle life of the electrodic material, can be checked.

1.2. EDXD Technique. The result of a conventional X-ray diffraction measurement is a curve of the diffracted intensity as a function of the scattering angle (2ϑ). However, a curve of this kind (diffractogram) requires the specification of the X-ray beam wavelength utilized for diffracting. If the wavelength is changed, the diffractogram undergoes a nonlinear stretching.

In contrast, it is possible to make a "universal" diffractogram by expressing the diffracted intensity as

(1) Scrosati, B. *Nature* **1995**, *373*, 557.
(2) Megahed, S.; Scrosati, B. *J. Power Sources* **1994**, *51*, 79.
(3) Megahed, S.; Scrosati, B. *Interface*, **1995**, *4* (4) 34.
(4) Vincent, C. A. V.; Scrosati, B. *Modern Batteries*; Arnold Pu: London, 1997.
(5) Wakihara, M.; Yamamoto, O. *Lithium Ion Batteries;* Kodasha Pu: Tokyo, 1998.

10.1021/cm0011007 CCC: $20.00
Published on Web 01/12/2001

a function of the "scattering parameter," q, the only variable on which the diffracted intensity actually depends. When expressed in terms of q, instead of 2ϑ, all of the diffractograms taken using X-rays of any wavelength will overlap. According to the theory of the elastic X-ray scattering,[6] q is the magnitude of the momentum (measured in $\hbar$ units) transferred from the radiation to the crystal lattice. By taking into account that the refraction index equals practically 1 in every material, q can be expressed as follows:

$$q = \alpha E \sin \vartheta \qquad (1)$$

where

$$\alpha = \frac{2}{hc} = 1.014 \text{ Å}^{-1} \text{ keV}^{-1}$$

Therefore, two ways to collect a diffraction pattern are possible, namely, either using a monochromatic radiation (E fixed) and scanning the diffraction angle (the conventional angular dispersive X-ray diffraction, ADXD), or using a continuous spectrum X-ray beam, called polychromatic or "white", leaving the angle unchanged during the measurement. This latter technique is called energy dispersive X-ray diffraction (EDXD).[7]

In laboratory ADXD, a fluorescence line of the X-ray source anode is used as the probe, after being selected by a monochromator. In EDXD, the Bremmstrahlung radiation emitted by the same anode is utilized, no monochromatization being required. In the former case, the q scan is performed mechanically by rotating the diffractometer arms, whereas, in the latter, the E scan is executed by a solid-state detector connected to a multichannel analyzer that is able to distinguish the energies of the scattered photons, no movement being needed.[8]

1.3. EDXD Applied to Electrodic Materials. An electrochemical cell, even in the simplified form used for in situ studies, is a complex object from the diffraction point of view. Usually, samples submitted to diffraction are held inside containers whose walls either do not contribute at all to the diffraction itself or, if they do, their contribution can be easily measured independently and subtracted from the overall diffracted intensity. To obtain this, the shape of the container must be extremely simple, generally a parallelepiped placed so that two of its faces are perpendicular and the other four are parallel to the X-ray beam when the scattering angle ϑ is zero. Unfortunately, the electrochemical and design constraints impose complex cell shapes and the simultaneous presence of several parts in addition to the electrodic material under investigation. A possible choice may be that of performing the X-ray measurements ex situ, i.e., interrupting the electrode operation at a certain stage and examining it after its removal from the cell. This means that the mounting of the cell must be repeated as many times as the number of samplings of the changing structure.

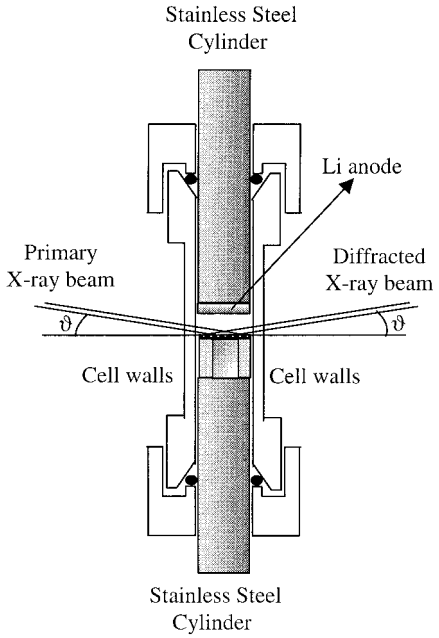

Figure 1. Schematic picture of the experimental electrochemical cell.

The best solution is to carry out in situ real-time measurements, but in this case, the cell must be conceived in such a way that the undesired effects concomitant with the X-ray diffraction of electrodic materials are minimized.

In ADXD, these effects basically consist of signal reduction due to the strong X-ray absorption of materials at the typical energies of the fluorescence radiations used for diffracting, i.e., 8.04 keV for Cu (Kα), 17.5 keV for Mo (Kα) and 24.5 keV for Ag (Kα). Higher energies would require a higher power supply voltage to obtain fluorescences of acceptable intensity. To overcome the absorption inconvenience, asymmetric geometries of the cells have been proposed as well as the use of Be windows [9] and an extreme reduction of the thickness (down to 20 μm) of the electrolytic solution layer through which the beam passes.[10] All of these expedients solved the problem only partly (Be is unstable at high voltages), and in some cases, their application may compromise the correct electrochemical behavior of the battery. Recently, the use of plastic batteries in coin-type containers has been successfully applied, but the diffraction is carried out on the external face of the working electrode.[11]

The different approach we propose is based on the well-known characteristics of the high-energy radiation used in EDXD.[12] In this case, no particular care is required for the measurement, and a simple polymeric tube filled with liquid electrolyte can be used (Figure 1). In fact, in EDXD the upper limit (E_{max}) of the Bremmsstrahlung energy spectrum corresponds to the power supply voltage of the tube and can reach rather high values. For example, if the supply voltage is 55

(6) James, R. W., Ed. *The Optical Principles of the Diffraction of X-rays*; Ox Bow Press: Oxford, 1982.
(7) Giessen, B. C.; Gordon, G. E. *Science* **1968**, *159*, 973.
(8) Caminiti, R.; Rossi Albertini; V. *Int. Rev. Phys. Chem.* **1999**, *18*, 263.
(9) Nahle′, A. H.; Walsh, F. C.; Brennan, C.; Roberts, K. J. *J. Appl. Crystallogr.* **1999**, *32*, 369.
(10) Robinson, K. M.; O'Grady, W. E. *Rev. Sci. Instr.* **1993**, *64* (4), 1061.
(11) Richard, M. N.; Koetschau, I.; Dahn, J. R. *J. Electrochem. Soc.* **1997**, *144*, (4), 554.
(12) Ronci, F.; Scrosati, B.; Rossi Albertini, V.; Perfetti, P. *Electrochem. Solid State Lett.* **2000**, *3*, 4.

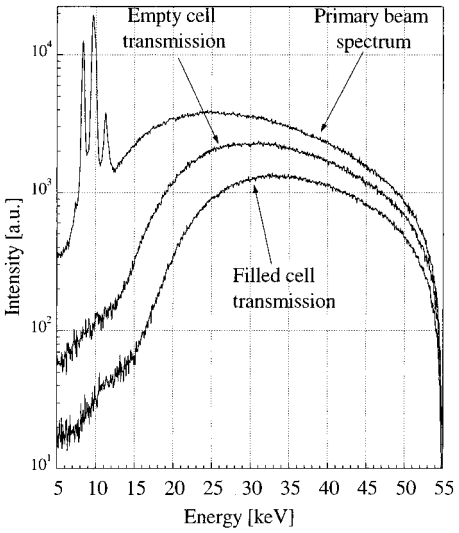

Figure 2. Comparison among the energy spectrum of the primary beam, of the radiation transmitted by the empty cell, and that transmitted by the cell filled with the electrolytic solution. It can be noticed that the strong fluorescence L-lines emitted by the W anode in the range 8−13 keV are completely absorbed.

kV (as in our case), the spectrum contains photons up to 55 keV. From the energy spectra reported in Figure 2, it can be noted that, at high energy, a remarkable portion of the incident radiation is transmitted. However, as the X-ray energy decreases, the cell becomes rapidly opaque so that the very intense fluorescence peaks in the (8−13) keV range are completely suppressed, even considering the cell walls absorption only. Therefore, diffraction measurements on cells of this kind could hardly be performed even using a high brilliance synchrotron radiation, when its energy (as often) is comparable with that of the fluorescence lines produced by laboratory sources.[13]

Moreover, EDXD is carried out without any motion of instrument parts. This guarantees a simplification of the geometrical arrangement and reduces the consequences of possible misplacements due to an imperfect pointing of the sample. In fact, because the angle is fixed, if the sample is misplaced in a EDXD measurement, the diffractogram undergoes a rigid shift, i.e., the same shift for all of the peaks. This shift can be easily corrected, for instance, by knowing the true position of one of the peaks. Instead, in ADXD, if the sample is vertically misplaced, the error will be different at different angles, inducing an angular dependent shift of the peaks.

Finally, according to eq 1, the highest q value scanned during diffraction is, in ADXD, $q_{max} \cong E_0 \sin \vartheta_{max}$ where E_0 is the fixed energy, whereas in EDXD $q_{max} \cong E_{max} \sin \vartheta_{max}$. Being the ratio between E_{max} and E_0 up to 3−4 (if the Mo[Kα] is used), the EDXD can scan a q space that is 3−4 times wider (and even 7 times when an usual copper anode is used).[8]

The main drawback of the EDXD technique is the poor resolution of the solid-state detector that causes a broadening of the peaks in the collected diffractogram. The relative error on q can be calculated from the logarithmic derivative of eq 1. It is higher than in ADXD due to the presence of the additional energetic term in the right-hand side of the equation:

$$\frac{\Delta q}{q} \cong \coth(\vartheta)\cdot\Delta\vartheta + \frac{\Delta E}{E}$$

Despite this, it will be shown that the loss in resolution is not a major problem and that very accurate results can be obtained using in situ EDXD.

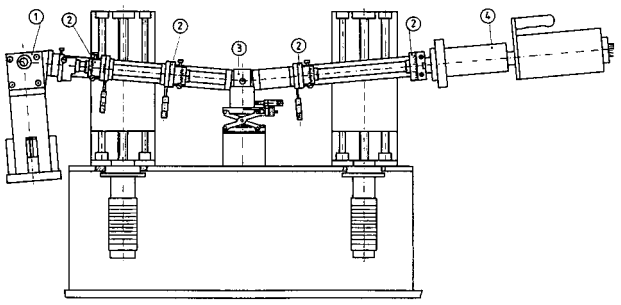

Figure 3. Drawing of the energy dispersive diffractometer used for these measurements, whose fundamental components are (1) an X-ray source (W anode tube), (2) collimation slits, (3) a sample holder, and (4) a Ge single-crystal energy-sensitive detector.

2. Experimental Section

The electrode membrane, cast on a 10 μm-thick Al foil, is composed by the intercalation material, $LiNi_{0.8}Co_{0.2}O_2$ (Merck) blended with a binder, polyethylene-copropylene-*co*-5-methylene-2 norbornene, EPDM (Aldrich), and a carbon powder, Super P (MMM Carbon Belgium), which guarantees the electronic conduction in the membrane. The weight ratio of the components was, respectively, 93:2:5. The electrochemical cell we used is shown in Figure 1. The cell container is formed by a 2 mm-thick cylindrical polyethylene tube, with a 10 mm inner diameter. The two stainless steel cylinders act as current collectors for the counter and working electrodes. The former consists of a high-purity Li foil, whereas the latter is the cathodic membrane itself, fixed on a plastic spacer, and kept in electronic contact with the current collector by means of the Al foil. A 1 M solution of $LiClO_4$ in ethylenecarbonate (EC)/dimethyl carbonate (DMC) (1:1 in weight) was poured in the cell container before it was sealed.

The energy dispersive X-ray diffractometer, shown in Figure 3, is a noncommercial instrument equipped by a W anode X-ray tube (Philips, model PW 2214/20), supplied at HV = 55 kV, I = 28 mA. The (nonmonochromatized) radiation emitted by it reaches the center of rotation of the diffractometer arms, where the sample is placed, after being collimated by two W slits mounted on the first arm. The other two slits of the second arm select the portion of the diffracted beam contained in the acceptance angle of the energy dispersive detector (EG&G, model 10180/07-p). The active part of the detector is a ultrapure Ge diode. When a photon is absorbed, the detector sends a signal to the computer by means of an electronic chain composed of an amplifying stage, a multichannel analyzer and an analog−digital converter. In the computer, the processed signal is used to plot the frequency histogram of the number of collected photons as a function of their energy. In this way, photon by photon, the energy spectrum of the diffracted radiation can be reconstructed and then stored in the computer memory.

2.1. Experimental Method. To illustrate the procedure adopted to measure the structural changes of the electrodic material the Murata, Nishikawa, and Iijima[14,15] instrumental

(13) Thurston, T. R.; Jisrawy, N. M.; Mukerjee, S.; Yang, X. Q.; McBreen, J.; Daroux, M. L.; King, X. K. *Appl. Phys. Lett.* **1996**, *69*, 194.

(14) Murata, Y.; Nishikawa, K. *Bull. Chem. Soc. Jpn.* **1978**, *51*, 411.
(15) Nishikawa, K.; Iijima, T. *Bull. Chem. Soc. Jpn.* **1984**, *57*, 1750.

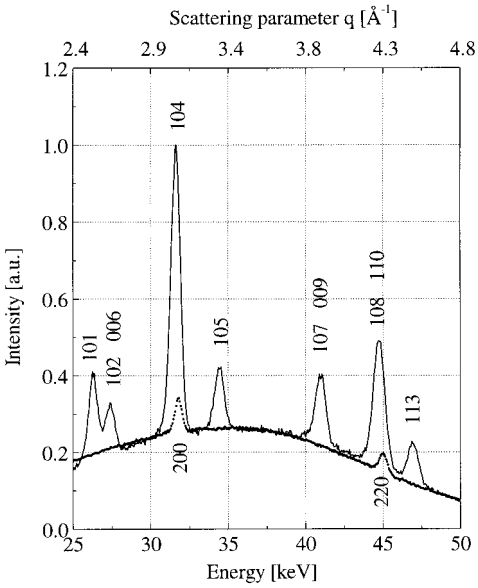

Figure 4. Energy profiles of the first diffraction pattern collected (solid line, I_2 of eq 4b) and of the signal coming from the cell without electrodic material (dot line, I_1 of eq 4a).

equation of the EDXD in the transmission geometry can be used. This equation is more complex than that of ADXD, and consequently, a longer data processing is required. In the single scattering approximation, it is as follows:

$$I_{obs}(E,\vartheta) = k(\vartheta)I_0(E)A(E,\vartheta)P(E,\vartheta)I_{scatt}(E,\vartheta) \quad (2)$$

where I_{obs} is the observed intensity, k is a normalization constant dependent on the scattering geometry, A is the X-ray absorption coefficient, P is the polarization of the scattered beam, and I_{scatt} is the total single scattered intensity.

Equation 2 applies when only the sample is irradiated. Consequently, modifications are required to take into account the effects of all of the objects interacting with the X-ray beam.

The demonstration of the correctness of our assumption will be given afterward. It will be shown how, after data processing, the signal produced by the electrode active material can be isolated from other contributions and overlaps with the diffractogram produced by the same substance measured alone. This means that, despite the effects (X-ray scattering and absorption) due to the other components of the cell (walls, electrolytic solution, metallic current collector), which modify and deform the observed intensity profile, it is possible to distinguish the diffraction from the sample.

Equation 2 can be rewritten for (1) a cell containing the Al current collector and filled by the electrolytic solution but without sample and (2) a cell also containing the sample:

$$I_1(E,\vartheta) = kI_0A_{cell}A_{Al}P[I_{cell} + I_{Al}] \quad (3a)$$

$$I_2(E,\vartheta) = kI_0A_{cell}A_{Al}A_{sam}P[I_{cell} + I_{Al} + I_{sam}] \quad (3b)$$

where the indexes of I and A (i.e., cell, Al, and sam) refer, respectively, to the cell, the Al holder, and the sample.

For the sake of simplicity, the angular parameter ϑ (unchanged during the measurements) and the independent variable E have been omitted in the right-hand member. The energy spectra of I_1 and I_2 are shown in Figure 4. In these measurements the scattering angle was chosen as $\vartheta = 5.48°$. Therefore, the useful energy interval 25−50 keV, where the absorption is not too high (see Figure 2), corresponds to a q range of about 2.4−4.8 Å^{-1}. In such a q range, several peaks are visible, allowing a precise determination of the lattice parameters.

In eqs 3, A_{cell} can be rendered explicitly as the product of $A_{sol}A_{walls}$, namely, the X-ray absorption due to the electrolytic solution and to the cell walls. Analogously, I_{cell} can be expressed by the sum $I_{sol} + I_{walls}$.

The aim is to isolate the term I_{sam} by rendering it explicitly with respect to known quantities. Once it is done, the profile of I_{sam} as a function of q is the diffractogram of the sample only, from which the information on its crystalline structure at the moment of the measurement can be gained. To do this, the quantities present in eq 3 must be analyzed.

(1) k is not relevant, because it is just a scaling factor that does not modifies the relative heights of a diffractogram peaks (namely, we will obtain kI_{sam} as the result of this procedure).

(2) I_0 can also be measured independently. Its intensity spectrum is shown in Figure 2.

(3) P can be calculated using the tables of the polarization coefficients.[8]

(4) A_{cell} can be easily calculated starting from a prior direct transmission measurement of the cell, consisting of placing the cell filled by just the solution into the center of the diffractometer, whose arms are set in horizontal position ($\vartheta = 0$). The ratio between the incident and the transmitted X-ray intensity provides $A_{cell}(E, \vartheta = 0)$. In this way, the quantity $A_{cell}(E, \vartheta)$ of eqs 3, which equals $[A_{cell}(E, \vartheta = 0)]^{1/\cos\vartheta}$, can be obtained.[14]

(5) A_{Al} is negligibly small, since the 10 μm-thick Al foil is practically transparent in the energy range of interest.

(6) Unlike A_{cell}, A_{sam} cannot be measured in the same simple way. In fact, due to the hybrid geometry of the cell, the cell walls and the solution within are in the transmission configuration, whereas the sample is in the reflection one. In the former, the length of the optical path does not depend on the point where the beam is scattered, whereas in the latter does,[8] and no simple relation as in A_{cell} applies. To solve the problem, usually approximated models or computer simulations are used. Instead, we preferred to obtain it by comparing eq 3a with eq 3b, taking advantage of their analytical form and of the characteristics of their terms.

Removing the Bragg peaks that constitute the quantities I_{sam} and I_{Al}, by a nonlinear fit of the background, it is possible to eliminate them from eq 3. This is quite easy since the term $I_{cell} = I_{sol} + I_{walls}$ represents the scattering of microscopically disordered objects (a liquid and an amorphous plastic) that do not produce sharp lines but just a characteristic hunch-shaped background.[16] Therefore, A_{sam} is simply the ratio I_2/I_1 after the elimination of the Bragg peaks.

In conclusion, after simple calculations, the I_{sam} q spectrum representing the powder diffractogram is obtained:

$$kI_{sam} = \frac{1}{I_0A_{cell}P}\left[\frac{I_2}{A_{sam}} - I_1\right] \quad (4)$$

In Figure 5, a comparison between kI_{sam}, namely, the diffraction signal coming from the powder as extracted by the overall signal of the cell, and the diffractogram of the same powder alone is made. The agreement is satisfactory, demonstrating that it is possible to focus the real-time changes of the powder despite the presence of all of the other scattering objects contained in the cell. The small discrepancies observable in the two curves of Figure 5 can be easily justified by taking into account the different experimental conditions in which the diffracted intensity are collected. The cell does not allow a fine positioning, so that the irradiated quantity of sample is different in the two cases and, likely, is observed under a different effective diffraction angle. The diffractogram of the powder in the cell shows a slightly lower resolution, as can be noticed looking at the double peak in the energy range 25−28 keV and at the major peak at about 32 keV. However, such discrepancies produce negligible differences in the lattice parameters values obtained by fitting the two diffractograms.

(16) Rossi Albertini, V.; Bencivenni, L.; Caminiti, R.; Cilloco, F.; Sadun, C. *J. Macromol. Sci.- Phys.* **1996**, *B35* (2), 199.

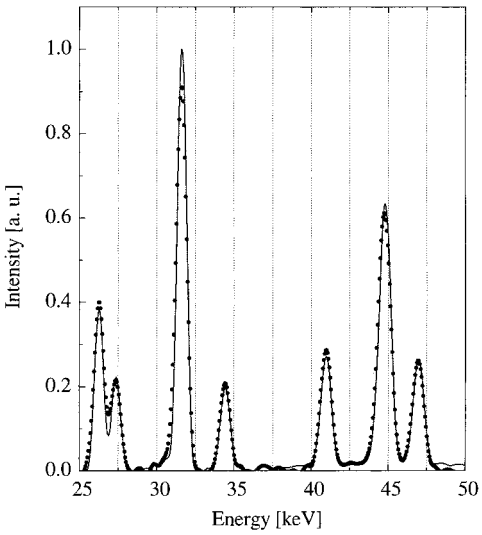

Figure 5. Comparison between the diffractograms of the electrodic material measured alone in the best conditions for powder diffraction (solid line) and after extraction from the overall signal coming from the cell, according to the model discussed in section 2.1 (dots). Both the curves were slightly smoothed to improve their visibility. The remarkable width of the peaks is mainly due to the magnification of the narrow q range of interest.

3. Results and Discussion

As an application of what discussed in the previous sections, a sequence of diffractograms produced by the $LiNi_{0.8}Co_{0.2}O_2$ cathodic material during its lithium release and uptake cycling was collected and then processed accordingly. The anodic and cathodic limits were set at 4.5 and 3.1 V, respectively, and the current at 22.8 μA for both charge (lithium deintercalation) and discharge (lithium intercalation). Such a low current corresponds to a C/72 theoretical charge and discharge rate (i.e., the time needed for the process of total deintercalation or intercalation, respectively, is 72 h). This rate guarantees the achievement of thermodynamic quasi-equilibrium conditions because of the low overvoltage produced by the dynamic process and, in addition, the homogeneity of the material structure, since it allows enough time to get lithium uniformly distributed inside the host lattice.

Three cycles of this kind were executed, with 1 h being the acquisition time of each diffractogram with a total duration of the experiment of about 270 h.

Considering that the chosen scattering angle ϑ was 5.48°, the useful energy interval (25−50) keV, where the absorption is not too high (see Figure 2), corresponds to a q range of about 2.4−4.8 $Å^{-1}$, as discussed in section 2.1.

Figure 6 shows a selection of the diffractograms collected during the first charge of the cell, as they appear after being processed and slightly smoothed to improve the visibility of the graph. Shifts of the peaks and changes in their intensities are evident. According to what was reported in the literature,[17] $LiNi_{0.8}Co_{0.2}O_2$ does not show phase changes upon cycling if full deintercalation is avoided. As a consequence, each diffractogram was precisely fitted by the PowderCell software using the initial $R\bar{3}m$ space group, a rhombohedral system with a layered structure ($a = b \neq c$ and $\alpha = \beta = 90°$, $\gamma = 120°$) and the time evolution of the lattice parameters was obtained. In Figure 7, these parameters are plotted together with the intercalation degree (x in $Li_xNi_{0.8}Co_{0.2}O_2$) and the cell voltage as a function of time.

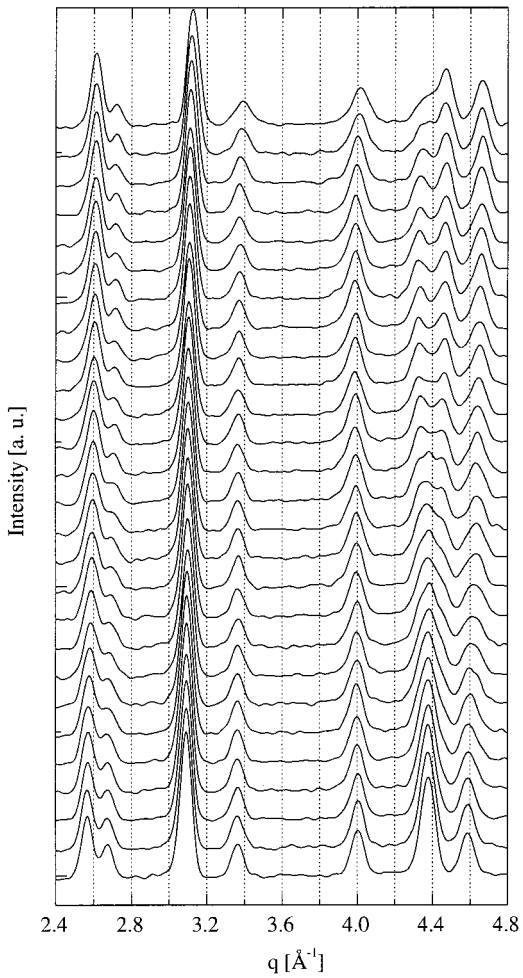

Figure 6. Selection of the diffractograms collected during the first charge of the cell (from the bottom to the top) to show the evolution of the electrodic material structure.

As expected, the profiles of the two curves during the first cycle (t < 122 h) are different from those of the following two cycles (122 < t < 196 h and 196 < t < 270 h). This is due to the well-known partial irreversibility of the first cycle, while only minor differences can be observed in the subsequent cycles.[18,19]

A remarkable feature of the a and c curves in Figure 7 is that, while the former oscillates having the same period and phase as the Li^+ intercalation degree x curve, the latter has the same period but is not simply in antiphase. This is the typical behavior of this class of intercalating compounds, as it was reported in several in situ ADXD works on $LiNiO_2$ [20] and $LiCoO_2$.[21,22] Since

(17) Levi, E.; Levi, M. D.; Salitra, G.; Aurbach, D.; Oesten, R.; Heider, U.; Heider, L. *Solid State Ionics* **1999**, *126*, 97.

(18) Delmas, C.; Saadoune, I.; Rougier, A. *J. Power Sources* **1993**, *43−44*, 595.

(19) Saadoune, I.; Delmas, C. *J. Mat Chem*, **1996**, *6* (2), 193.

(20) Li, W.; Reimers, J. N.; Dahn, J. R. *Solid State Ionics* **1993**, *67*, 123.

(21) Reimers, J. N.; Dahn, J. R. *J. Electrochem. Soc.* **1992**, *139* (8), 2091.

(22) Amatucci, G. G.; Tarascon, J. M.; Klein, L. C. *J. Electrochem. Soc.* **1998**, *143*, 1114.

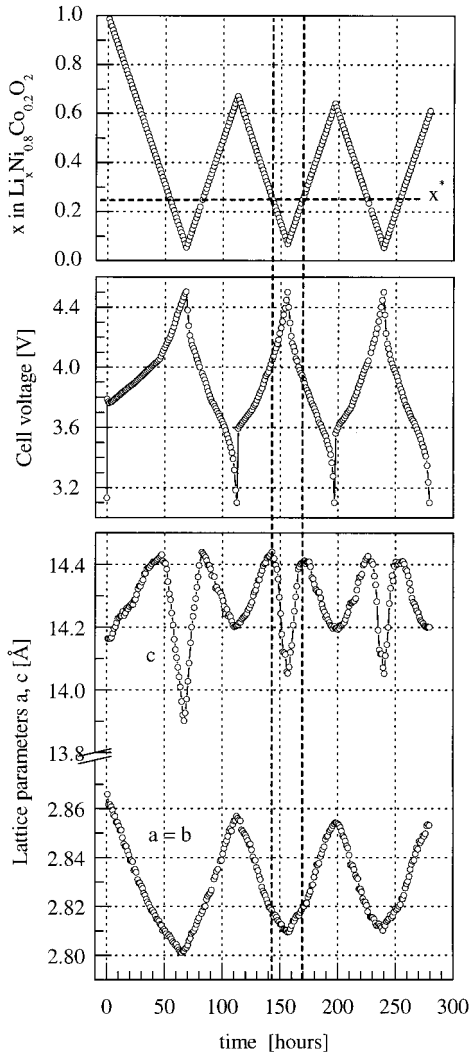

Figure 7. Real-time change of the cell voltage and of the lattice parameters as a function of with the intercalation degree *x*. The critical value *x** is reported.

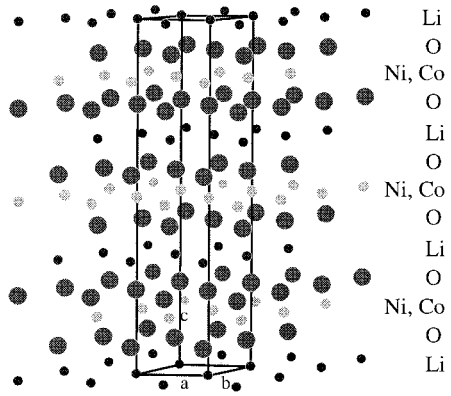

Figure 8. Crystallographic structure of the fully intercalated $LiNi_{0.8}Co_{0.2}O_2$ electrodic material (pristine state).

many peaks are contained in the observed *q* range (Figure 4), and they are all utilized simultaneously in the fit, the accuracy of the measurement is good. Therefore, although the resolution of EDXD is poorer than that of the conventional diffraction, the statistical noise of the experimental points in the a and c curves is small, and all of the features of the curves can be clearly seen.

The crystallographic structure of $LiNi_{0.8}Co_{0.2}O_2$ is schematically depicted in Figure 8. In this structure, the *a* and *b* parameters are connected to the ion distances along the two in-plane lattice directions, whereas *c* depends on the distance in the off-plane direction.

This layered material, in the pristine state, can be regarded as formed by strongly bonded O−M−O slabs (where M = Ni, Co) separated by Li^+ planes. Due to the weaker interaction between Li^+ ions and the O−M−O slabs, the Li^+ ions can move from their sites through the plane and deintercalate from the host structure.

The *a* parameter curve show a monotonic decrease during charge (Li^+ deintercalation), due to the progressive oxidation of the transition-metal ions, with consequent decrease of their ionic radii. This behavior is different from what was reported for the parent compounds $LiNiO_2$ [20] and $LiCoO_2$.[21,22]

The *c* parameter curve shows an initial increase as *x* decreases until a certain threshold value *x** is reached. Excluding the first cycle, which shows partially irreversible effects, in the subsequent two cycles, *x** maintains a constant value of about 0.25. Continuing the charging process, for *x* values lower than *x**, the *c* parameter begins to drop rapidly, reaching its minimum in correspondence to the anodic (highest) voltage limit. This trend is due to two concomitant effects. The first one is the lithium ions' deintercalation, which causes an initial increase in the repulsion between adjacent O−M−O slabs, and the second is the progressive oxidation of the transition-metal ions which progressively reduces the repulsion, decreasing the net charge of the O−M−O slabs. In this view, the critical *x** value can be regarded as that value at which the two opposite tendencies are balanced.

The part of the c curve relative to the discharge process shows a specular trend, confirming the reversibility of the process in each cycle.

Conclusions

We presented an experimental procedure based on energy dispersive X-ray diffraction to follow in situ real-time changes of electrodic materials and discussed the way to correct and process the experimental data.

The method was successfully applied to the $LiNi_{0.8}Co_{0.2}O_2$ cathode material for Li-ion batteries and provided a rich and detailed description of its lattice parameters time evolution.

Therefore, the proposed EDXD technique turned out to be a reliable and accurate method for laboratory in situ diffraction studies, and its application may be of use for a systematic study of the electrodic materials in all of the numerous experimental conditions in which a cell may operate.

Acknowledgment. Sincere thanks are expressed to Mr. Massimo Brolatti and Mrs. Daniela de Fazio for their valuable help in the solution of technical and practical problems of the X-ray laboratory.

CM0011007